

Induced Violation of Time-Reversal Invariance in the Regime of Weakly Overlapping Resonances

B. Dietz,¹ T. Friedrich,^{1,2} H. L. Harney,³ M. Miski-Oglu,¹

A. Richter,^{1,4,*} F. Schäfer,¹ J. Verbaarschot,⁵ and H. A. Weidenmüller³

¹*Institut für Kernphysik, Technische Universität Darmstadt, D-64289 Darmstadt, Germany*

²*GSI Helmholzzentrum für Schwerionenforschung GmbH, D-64291 Darmstadt, Germany*

³*Max-Planck-Institut für Kernphysik, D-69029 Heidelberg, Germany*

⁴*ECT*, Villa Tambosi, I-38050 Villazzano (Trento), Italy*

⁵*Department of Physics and Astronomy,
SUNY at Stony Brook, NY 11794, USA*

(Dated: March 18, 2019)

Abstract

We measure the complex scattering amplitudes of a flat microwave cavity (a “chaotic billiard”). Time-reversal (\mathcal{T}) invariance is partially broken by a magnetized ferrite placed within the cavity. We extend the random-matrix approach to \mathcal{T} violation in scattering, fit some of the properties of the scattering amplitudes, and then successfully predict others. Our work constitutes the most precise test of the theoretical approach to \mathcal{T} violation within the framework of random-matrix theory so far available.

PACS numbers: 24.60.Ky, 05.45.Mt, 11.30.Er, 85.70.Ge

We measure the violation of time-reversal (\mathcal{T}) invariance in the excitation functions of a flat microwave cavity (a “chaotic microwave billiard”) due to a magnetized ferrite placed within the cavity. The data is used to test a random-matrix approach to \mathcal{T} -invariance violation in scattering processes. In random-matrix theory (RMT) the N -dimensional Hamiltonian matrix H of the system (the cavity) is written as the sum of two parts [1, 2], $H = H^s + i(\pi\xi/\sqrt{N})H^a$. The real, symmetric, and \mathcal{T} -invariant matrix H^s is taken from the Gaussian Orthogonal Ensemble (GOE) of random matrices while the real antisymmetric random matrix H^a with Gaussian-distributed matrix elements models the \mathcal{T} -invariance breaking part of H . For $N \rightarrow \infty$, \mathcal{T} invariance is significantly broken when the dimensionless parameter is close to unity [3]. Although widely used (to discover signatures of \mathcal{T} violation in compound-nucleus reactions [4] in the Ericson regime [5], to describe electron transport through mesoscopic samples in the presence of a magnetic field [6], and in ultrasound transmission in rotational flows [7]) this generic model of \mathcal{T} violation has, to the best of our knowledge, never been exposed to a detailed experimental test. The present work fills that gap.

Chaotic billiards have been used before to study the effect of \mathcal{T} -invariance violation on the eigenvalues [8, 9, 10], on the eigenfunctions [11], and on the scattering due to isolated and nearly degenerate resonances [12]. We use the fluctuations with energy of the scattering matrix to test analytic results which we obtained based on the RMT approach in the regime of weakly overlapping resonances where the average level spacing is of the order of the resonance width.

Experiment. The flat copper microwave resonator has the shape of a tilted stadium [13] (see Fig. 1) and a height of 5 mm. For frequencies f up to 30 GHz the resonator simulates a

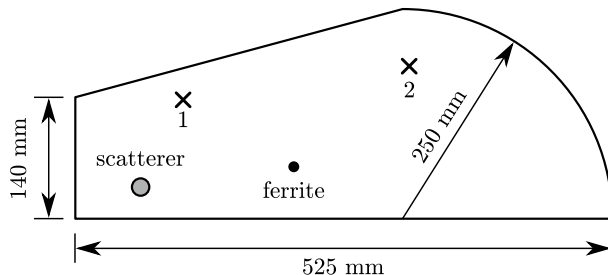


FIG. 1: The tilted stadium billiard (schematic). The two antennas 1, 2 connect the resonator to the VNA. The ferrite is fixed, the scatterer can be moved freely.

two-dimensional quantum billiard [14]. An Agilent PNA-L N5230A vector network analyzer (VNA) coupled rf energy via one of two antennas labeled 1 and 2 into the resonator and determined magnitude and phase of the transmitted (reflected) signal at the other (same) antenna in relation to the input signal and, thus, the elements $S_{ab}(f)$ with $a, b = 1, 2$ of the complex-valued 2×2 scattering matrix $S(f)$. Distorting effects of the connecting coaxial cables were removed by calibration. We measured the elements of $S(f)$ in the frequency range 1–25 GHz at a resolution of 100 kHz. To improve the statistical significance of the data set, an additional scatterer (an iron disc of 20 mm diameter) was placed within the cavity. It could be freely moved and allowed the measurement of statistically independent spectra, so-called “realizations”.

Time-reversal invariance is violated by a ferrite cylinder ($4\pi M_S = 1859$ Oe, $\Delta H = 17.5$ Oe, courtesy of AFT Materials GmbH, Backnang, Germany) of 4 mm diameter and 5 mm height. The cylinder was embedded inside the resonator and magnetized by an external magnetic field B . The field was provided by two NdFeB magnets (cylindrical shape, 20 mm diameter and 10 mm height) attached from the outside to the billiard. Field strengths of up to 360 mT could be attained. Here we focus on the results at $B = 190$ mT as there the effects are most clearly visible. The spins within the ferrite precess collectively with their Larmor frequency about the external field. The rf magnetic fields of the resonator modes are, in general, elliptically polarized and couple to the spins of the ferrite. The coupling depends on the rotational direction of the rf field. An interchange of input and output channels changes the rotational direction and thus the coupling of the resonator modes to the ferrite. Figure 2 demonstrates that reciprocity, defined by $S_{12}(f) = S_{21}(f)$ and implied by \mathcal{T} invariance, is violated.

As a measure of the strength of \mathcal{T} -invariance violation, we define the cross-correlation coefficient $C_{\text{cross}}(\epsilon = 0)$ where

$$C_{\text{cross}}(\epsilon) = \frac{\Re(\langle S_{12}(f) S_{21}^*(f + \epsilon) \rangle)}{\sqrt{\langle |S_{12}(f)|^2 \rangle \langle |S_{21}(f)|^2 \rangle}}. \quad (1)$$

If \mathcal{T} invariance holds, we have $C_{\text{cross}}(0) = 1$ while for complete breaking of \mathcal{T} invariance S_{12} and S_{21} are uncorrelated and thus $C_{\text{cross}}(0) = 0$. The average $\langle \cdot \rangle$ over the data is taken in frequency windows of width 1 GHz and over 6 realizations, i.e., positions of the additional scatterer. The upper panel of Figure 3 shows $C_{\text{cross}}(0)$ for the different frequency windows. The cross-correlation coefficient is seen to depend strongly on f although complete violation

of \mathcal{T} invariance is never attained. At 5–7 GHz the Larmor frequency of the ferrite matches the rf frequency, and the ferromagnetic resonance directly results in $C_{\text{cross}}(0) \approx 0.8$. Around 15 GHz the effects of \mathcal{T} -invariance violation are strongest, $C_{\text{cross}}(0) \approx 0.5$. A third minimum is observed at about 24 GHz. The connection of the latter two minima to the properties of the ferrite is not clear.

Analysis. We analyze the data with a scattering approach developed in the context of compound-nucleus reactions [15]. The scattering matrix for the scattering from antenna b to antenna a with $a, b = 1, 2$ is written as

$$S_{ab}(f) = \delta_{ab} - 2\pi i (W^\dagger (f - H^{\text{eff}})^{-1} W)_{ab}. \quad (2)$$

The matrix $W_{\mu a}$ is rectangular and describes the coupling of the N resonant states μ in the cavity with antenna a . We assume that \mathcal{T} -invariance violation is due to the ferrite only. Then $W_{\mu a}$ is real. The resonances in the cavity are modeled by $H^{\text{eff}} = H - i\pi \tilde{W} \tilde{W}^\dagger$. Here H is the Hamiltonian of the closed resonator. The elements of the real matrix $\tilde{W}_{\mu c}$ are equal to those of $W_{\mu c}$ for $c = 1, 2$. Additional fictitious channels c are introduced to mimic Ohmic absorption in the walls of the cavity and the ferrite [16]. The classical dynamics inside the tilted stadium billiard is chaotic. Therefore [17], we model H by an ensemble of random matrices as described in the first paragraph. In the limit $N \rightarrow \infty$, $C_{\text{cross}}(0)$ can be expressed analytically in terms of a threefold integral involving the parameter ξ . For the derivation we extended the method of Ref. [18] where the ensemble average of $|S_{ab}|^2$ was computed as function of the parameter ξ . The cross-correlation coefficient $C_{\text{cross}}(0)$ is obtained by setting

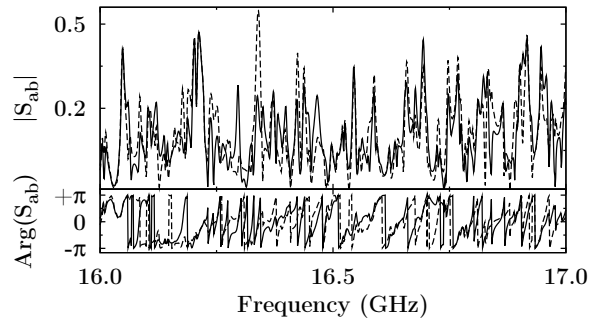


FIG. 2: Transmission spectra for $B = 190$ mT in the range 16–17 GHz. The amplitudes and phases of S_{12} (solid) and S_{21} (dashed) are seen to differ.

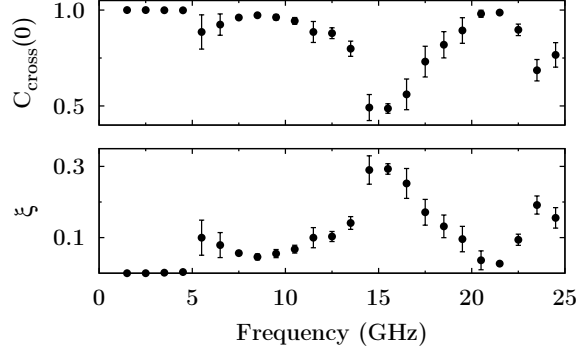


FIG. 3: Experimentally determined values of $C_{\text{cross}}(0)$ (upper panel) from Eq. (1) and the parameter ξ for \mathcal{T} -invariance violation deduced from these (lower panel) with the help of Eq. (3). The error bars indicate the r.m.s. variation of $C_{\text{cross}}(0)$ over the 6 realizations.

$\epsilon = 0$, $\sigma = -1$, and $a, b = 1, 2$ in the function

$$\begin{aligned}
F_{ab}^{\sigma}(\epsilon|T_a, T_b, \tau_{\text{abs}}, \xi) &= \frac{1}{8} \int_0^{\infty} dx_1 \int_0^{\infty} dx_2 \int_0^1 dx \\
&\times \frac{\mu(x, x_1, x_2)}{\mathcal{F}} \cdot \exp\left(-\frac{i\pi\epsilon}{d}(x_1 + x_2 + 2x)\right) \\
&\times \prod_c \frac{1 - T_c x}{\sqrt{(1 + T_c x_1)(1 + T_c x_2)}} \left[\left\{ J_{ab}(x, x_1, x_2) \right. \right. \\
&\times [\mathcal{F}\mathcal{E}_+ + (\lambda_2^2 - \lambda_1^2)\mathcal{E}_- + 4\mathfrak{t}\mathcal{R}(\lambda_2^2\mathcal{E}_- + \mathcal{F}(\mathcal{E}_+ - 1))] \\
&+ \sigma \cdot 2(1 - \delta_{ab})T_a T_b [\mathcal{E}_- K_{ab}(\lambda, \lambda_1, \lambda_2|T_a, T_b, \xi) \\
&+ \left(\mathcal{E}_+ - \frac{\mathcal{E}_-}{\mathfrak{t}\mathcal{F}}\right) L_{ab}(\lambda, \lambda_1, \lambda_2|T_a, T_b, \xi)] \left. \right\} \cdot \exp(-2\mathfrak{t}\mathcal{G}_-) \\
&+ (\lambda_1 \leftrightarrow \lambda_2) \Big], \tag{3}
\end{aligned}$$

with the notations

$$\begin{aligned}
\mathfrak{t} &= \pi^2 \xi^2, \quad \mathcal{R} = 4(x + x_1)(x + x_2), \\
\mathcal{U} &= 2\sqrt{x_1(1 + x_1)x_2(1 + x_2)}, \quad \mathcal{F} = 4x(1 - x), \\
\mathcal{E}_{\pm} &= 1 \pm \exp(-2\mathfrak{t}\mathcal{F}), \quad \lambda = 1 - 2x, \\
\lambda_i &= \sqrt{(1 + x_1)(1 + x_2) + x_1 x_2 - (-1)^i \mathcal{U}}, \\
\mathcal{G}_i &= \lambda_i^2 - 1, i = 1, 2. \tag{4}
\end{aligned}$$

The integration measure $\mu(x, x_1, x_2)$ and the function $J_{ab}(x, x_1, x_2)$ are given explicitly in Ref. [19], while the functions $K_{ab}(\lambda, \lambda_1, \lambda_2|T_a, T_b, \xi)$ and $L_{ab}(\lambda, \lambda_1, \lambda_2|T_a, T_b, \xi)$ can be read

off Eq. (2) of Ref. [20]. We checked our analytic results by numerical RMT simulations. The parameters of Eq. (3) for $\epsilon = 0$ are ξ , the transmission coefficients $T_a = 1 - |\langle S_{aa} \rangle|^2$ for $a = 1, 2$, and the sum τ_{abs} of 300 transmission coefficients for the additional, weakly coupled equivalent channels that model the Ohmic losses [16, 21]. The parameter τ_{abs} is fitted to the data, see below. We suppress these parameters in the notation $C_{\text{cross}}(0)$ for the cross-correlation function.

For a typical set $T_1, T_2, \tau_{\text{abs}}$, Fig. 4 shows $C_{\text{cross}}(0)$ versus ξ . Within the frequency range 1–25 GHz, $C_{\text{cross}}(0)$ depends very weakly on $T_1, T_2, \tau_{\text{abs}}$, and Fig. 4 can be taken to be universal. For each data point shown in the upper panel of Fig. 3 the corresponding value

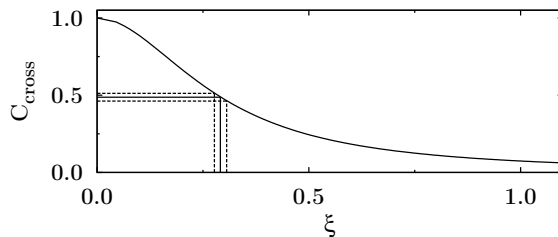


FIG. 4: Dependence of the cross-correlation coefficient $C_{\text{cross}}(0)$ on the parameter ξ as predicted by the random-matrix model for partial violation of \mathcal{T} invariance. Also shown is how $C_{\text{cross}}(0) = 0.49(3)$ translates into $\xi = 0.29(2)$.

of ξ was read off Fig. 4 and the result is shown as function of f in the lower panel of Fig. 3. Figure 3 shows that we are in the fortunate position to study S -matrix fluctuations over a wide range of parameters: In the interval from 1 to 25 GHz, the strength ξ of \mathcal{T} breaking varies from zero to 0.3, while the ratio of the average resonance width Γ to the average resonance spacing d varies from $\Gamma/d \approx 0.01$ to $\Gamma/d \approx 1.2$.

Autocorrelation function. Since $C_{\text{cross}}(0)$ depends only weakly on the values of T_1, T_2 and τ_{abs} , we used the autocorrelation function $C_{ab}(\epsilon)$ for a more precise determination of these parameters. The function

$$C_{ab}(\epsilon) = \langle S_{ab}(f) S_{ab}^*(f + \epsilon) \rangle - |\langle S_{ab}(f) \rangle|^2 \quad (5)$$

was calculated analytically with the method of Ref. [18] as a function of $T_1, T_2, \tau_{\text{abs}}, \xi$, and of d and is obtained from Eq. (3) by setting $\sigma = +1$. It interpolates between the well-known results for orthogonal symmetry [19] (full \mathcal{T} invariance) and for unitary symmetry [22]

(complete violation of \mathcal{T} invariance). The mean level spacing d was computed from the Weyl formula. The values for T_1, T_2 obtained from the data and ξ determined from $C_{\text{cross}}(0)$ were used as starting points for a fit of the autocorrelation function to the data based on the method developed in Ref. [21]. For each of the 6 realizations the spectra of $S_{ab}(f)$ were divided into intervals Δf of 1 GHz length. In each interval the Fourier transform $\tilde{C}_{ab}(t_k)$ of the autocorrelation function (5) was calculated for the times $t_k < 200$ ns. The time resolution was $1/\Delta f = 1$ ns. We measured four excitation functions $S_{ab}(f)$ taking $a, b = 1, 1$ and $a, b = 1, 2$ and $a, b = 2, 1$ and $a, b = 2, 2$; that yields a total of 4800 Fourier coefficients from each interval. At $t_k \approx 200$ ns the values of $\tilde{C}_{ab}(t_k)$ have decayed over more than three orders of magnitude, and noise limits the analysis. The spread of the data is large, see the left panel of Fig. 5. Going to the time domain is useful since the $S_{ab}(f)$ are correlated for neighboring f whereas the correlations are removed in the ratios of the experimental and the fitted values for $\tilde{C}_{ab}(t_k)$. The latter are stationary and fluctuate about unity. Thus the statistical analysis is much simplified.

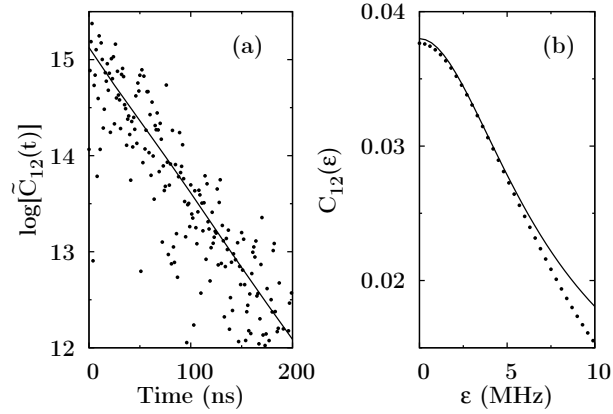


FIG. 5: Autocorrelation function for S_{12} in the range of 16–17 GHz and at $B = 190$ mT. In the time domain (a) the data (dots) scatter around the theoretical fit (solid) for $\xi = 0.246$. Transforming the results back into frequency domain (b) confirms the good agreement between data and theory. We observe that neighboring data points in (b) are correlated, whereas those in (a) are not.

For each realization the parameters $T_a, T_b, \tau_{\text{abs}}, \xi$ were obtained by fitting the analytical expression for $\tilde{C}_{ab}(t_k)$ to the experimental results. The values of ξ determined from these fits agree with the ones found from the cross-correlation coefficient. To reduce the spread we combined the data from all realizations within a fixed frequency interval. The result

was analyzed with the help of a goodness-of-fit (GOF) test (see Ref. [21]) that distinguishes between full, partial, and no violation of \mathcal{T} invariance. We defined a confidence limit such that the GOF test erroneously rejects a valid theoretical description of the data with a probability of 10 %. With this confidence limit the test rejects the fitted expressions for $\tilde{C}_{ab}(t_k)$ in only 1 out of the 24 available frequency windows or in 4.2 % of the tests. Thus, the RMT model correctly describes the fluctuations of the S -matrix for partial violation of \mathcal{T} invariance in the regimes of isolated and weakly overlapping resonances.

Elastic enhancement factor. As a second test of the theory we use the values of ξ obtained from the cross-correlation coefficients (see Fig. 3) and the parameters $T_a, T_b, \tau_{\text{abs}}$ resulting from the fit of $\tilde{C}_{ab}(t_k)$ to predict the values of the elastic enhancement factor $\mathcal{W} = \left(\langle |S_{11}^{\text{fl}}|^2 \rangle \langle |S_{22}^{\text{fl}}|^2 \rangle \right)^{1/2} / \langle |S_{12}^{\text{fl}}|^2 \rangle$ with $S_{\text{ab}}^{\text{fl}} = S_{\text{ab}} - \langle S_{\text{ab}} \rangle$ as a function of f . We use that $\mathcal{W} = \sqrt{C_{11}(0)C_{22}(0)}/C_{12}(0)$, see Eq. (5). For \mathcal{T} -invariant systems, the elastic enhancement factor decreases from $\mathcal{W} = 3$ for isolated resonances with many weakly coupled open channels to $\mathcal{W} = 2$ for strongly overlapping resonances ($\Gamma \gg d$). The corresponding values for complete violation of \mathcal{T} invariance are $\mathcal{W} = 2$ and $\mathcal{W} = 1$, respectively [23]. Figure 6 compares the analytic results for the enhancement factor \mathcal{W} (filled circles) to the data (open circles). At low frequency only few resonances contribute and thus the errors of the experimental values for \mathcal{W} are large. Moreover \mathcal{W} is determined from only a single value $C_{ab}(0)$ of the measured autocorrelation function. In contradistinction, the analytic result is based on a fit of the complete autocorrelation function. The figure shows that at low frequency (where $\Gamma/d \ll 1$ and $\xi \approx 0$) we have $\mathcal{W} = 3$. With increasing frequency Γ/d increases, and \mathcal{W} slowly decreases. At 5–6 GHz there is a small dip in \mathcal{W} caused by the ferromagnetic resonance. Around 16 and 23 GHz two further minima in \mathcal{W} are observed. All three minima match the increased violation of \mathcal{T} invariance seen in the cross-correlation coefficient. At those frequencies where ξ is largest, the enhancement factor drops below the value 2, a situation that cannot arise for \mathcal{T} -invariant systems. The good agreement between both data sets above ≈ 10 GHz corroborates the confidence in the values of ξ deduced from the cross-correlation coefficients.

Summary. We have investigated partial violation of \mathcal{T} invariance with the help of a magnetized ferrite placed within a flat microwave resonator with two antennas (a chaotic billiard). We measured reflection and transmission amplitudes in the regime of isolated and

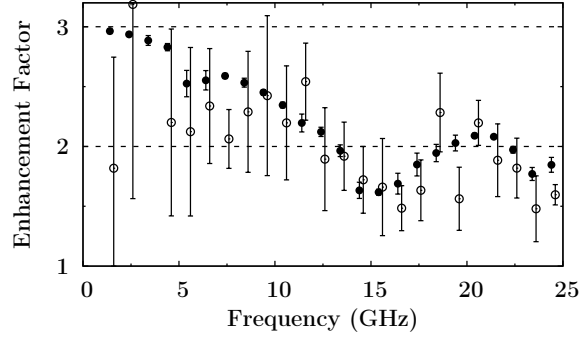


FIG. 6: Comparison of elastic enhancement factors. For the evaluation of \mathcal{W} the autocorrelation coefficients $C_{ab}(0)$ were determined either directly from the data (open circles) or from the analytic result for partial violation of \mathcal{T} invariance (filled circles) with ξ determined from the cross-correlation coefficient. The error bars indicate the variations within the 6 realizations. The dashed horizontal lines indicate the limits of \mathcal{W} for \mathcal{T} -invariant systems in the regime of isolated ($\mathcal{W} = 3$) or overlapping ($\mathcal{W} = 2$) resonances.

weakly overlapping resonances in the frequency range from 1 to 25 GHz and determined the cross-correlation function, the autocorrelation functions, and the elastic enhancement factor from the data. The results were used as a test of random-matrix theory with partial \mathcal{T} violation. That theory yields analytic expressions for all three observables. The parameters of the theory ($T_1, T_2, \tau_{\text{abs}}$ and the parameter ξ for \mathcal{T} violation) were fitted to both correlation functions. We find that $0 \leq \xi \leq 0.3$. The validity of the theory was then tested in two ways. (i) A goodness-of-fit test of the Fourier coefficients of the scattering matrix in frequency intervals of 1 GHz width yielded excellent agreement. (ii) The elastic enhancement factor theoretically predicted from the fitted values of the parameters agrees very well with the data, especially for frequencies above 10 GHz where the experimental errors are small. We conclude that the random-matrix description of S -matrix fluctuations with partially broken \mathcal{T} invariance is in excellent agreement with the data.

F. S. is grateful for the financial support from the Deutsche Telekom Foundation. This work was supported by the DFG within SFB 634.

* Electronic address: richter@ikp.tu-darmstadt.de

[1] A. Pandey, Ann. Phys. (N.Y.) **134**, 110 (1981).

- [2] A. Pandey and M. L. Mehta, Comm. Math. Phys. **87**, 449 (1983).
- [3] Time-reversal invariance is significantly broken for $\pi\xi/\sqrt{N} \simeq d/v$. Here, $d = v\pi/\sqrt{N}$ denotes the average level spacing and v^2 the variance of the off-diagonal matrix elements of H^s , H^a .
- [4] W. von Witsch, A. Richter, and P. von Brentano, Phys. Rev. Lett. **19**, 524 (1967); E. Blanke *et al.*, ibid. **51**, 355 (1983).
- [5] T. Ericson, Phys. Rev. Lett. **5**, 430 (1960).
- [6] G. Bergman, Phys. Rep. **107**, 1 (1984).
- [7] J. Rosny *et al.* Phys. Lett. **95**, 074301 (2005).
- [8] P. So, S. M. Anlage, E. Ott, and R. N. Oerter, Phys. Rev. Lett. **74**, 2662 (1995).
- [9] U. Stoffregen *et al.*, Phys. Rev. Lett. **74**, 2666 (1995).
- [10] O. Hul *et al.*, Phys. Rev. E **69**, 056205 (2004).
- [11] D. H. Wu, J. S. A. Bridgewater, A. Gokirmak, and S. M. Anlage, Phys. Rev. Lett. **81**, 2890 (1998).
- [12] B. Dietz *et al.*, Phys. Rev. Lett. **98**, 074103 (2007).
- [13] H. Primack and U. Smilansky, J. Phys. A **27**, 4439 (1994).
- [14] H.-J. Stöckmann and J. Stein, Phys. Rev. Lett. **64**, 2215 (1990).
- [15] C. Mahaux and H. A. Weidenmüller, *Shell-Model Approach to Nuclear Reactions* (North-Holland Publ. Co., Amsterdam, 1969).
- [16] P. W. Brouwer and C. W. J. Beenakker, Phys. Rev. B **55**, 4695 (1997).
- [17] O. Bohigas, M. J. Giannoni, and C. Schmitt, Phys. Rev. Lett. **52**, 1 (1984).
- [18] Z. Pluhař *et al.*, Ann. Phys. **243**, 1 (1995).
- [19] J. J. M. Verbaarschot, H. A. Weidenmüller, and M. R. Zirnbauer, Phys. Lett. B **149**, 263 (1984).
- [20] U. Gerland and H. A. Weidenmüller, Europhys. Lett. **35**, 701 (1996).
- [21] B. Dietz *et al.*, Phys. Rev. E **78**, 055204(R) (2008).
- [22] Y. V. Fyodorov, D. V. Savin, and H.-J. Sommers, J. Phys. A: Math. Gen. **38**, 10731 (2005).
- [23] D. V. Savin, Y. V. Fyodorov, and H.-J. Sommers, Acta Phys. Pol. A **109**, 53 (2006).